

10th CIRP Conference on Photonic Technologies [LANE 2018]

Surface functionalization under water using picosecond and femtosecond laser pulses – first observations and novel effects

Jürgen Koch^{a,*}, Sebastian Taschner^a, Oliver Suttmann^a, Stefan Kaierle^a

^aLaser Zentrum Hannover e.V., Hollerithallee 8, 30419 Hannover, Germany

* Corresponding author. Tel.: +49 511 2788-217; fax: +49 511 2788-100. E-mail address: j.koch@lzh.de

- Invited Paper -

Abstract

Functionalization by changing the topography of workpiece surfaces is interesting for many applications. Lasers – especially ultrashort pulse lasers – are flexible tools for this kind of tasks. Besides deterministic structures they allow for processing surfaces in a way that stochastic structures appear. Ripple and spike structures can be fabricated in air. In liquids, however, there are only a few investigations and many open questions. The idea of this paper is to check how water in contact to the workpiece surface affects femtosecond laser surface processing and what kind of structures appear. Results obtained with a picosecond laser are presented for comparison.

© 2018 The Authors. Published by Elsevier Ltd. This is an open access article under the CC BY-NC-ND license

(<https://creativecommons.org/licenses/by-nc-nd/4.0/>)

Peer-review under responsibility of the Bayerisches Laserzentrum GmbH.

Keywords: surface functionalization; ultrashort pulse laser; material processing in liquids; spike structures

1. Introduction

Nature has created a broad range of functional surface topographies whose implementation into technical applications is of great interest. Well-known examples are the water-repellent and self-cleaning lotus effect™, the flow loss-reducing sharkskin as well as the adhesion system of Gecko feet. While technical surfaces are often designed with the aim of minimizing roughness, in nature roughness is the key to functionality. Bionics tries to transfer surface functions from nature into technical applications. What is needed are techniques that are able to produce the generally micro- to nano-scale functional surface structures in an abstracted form following nature's example.

The technical implementation is faced with the challenge of producing structures with a resolution down to the submicron or even nanometer range relatively quickly and cost-effectively. The structures can include high aspect ratios

or undercuts. Applicability on non-planar components can be required.

The variety of different topography specifications and materials cannot be handled with a single processing technique. Many classic machining techniques such as milling, grinding and eroding often fail due to the required structure sizes. Also most additive processes are in this respect still fraught with almost insurmountable obstacles.

Material ablative laser processes have been increasingly used in recent years to produce functional surface topographies.[1] In particular, the ultrashort pulse lasers have distinguished themselves by their low-damage and spatially high-resolution processing options on almost all solid and gel-like materials. Structure sizes down to the deep submicron range can be realized.[2] The heat-affected zones remain so small that even very heat-sensitive materials can be processed. In addition to deterministic structures such as trenches, wells, etc. of widely differing dimensions, stochastic structures can also be generated. The latter are not exactly reproducible.

Characteristic structural dimensions such as average distances can be controlled by the laser parameters. The best known examples are ripple and spike structures. Ripple structures are also known as laser-induced periodic surface structures (LIPSS). An alternative common name for spike structures is cone-like protrusions (CLPs). Both types of structure do not require tight focusing of the laser beam. The structures are created when scanning surfaces with a laser focus which is much larger than the structures themselves. The topography of the spike structures – disordered microstructures with superimposed nanostructures – resembles the topography of the lotus leaf surface. The effect is the same: appropriately structured surfaces are water-repellent and self-cleaning.

Laser processing in liquids is done for mainly two reasons: cooling the workpiece and flushing away particles. A typical application is stent cutting with nanosecond lasers. For some applications there is a third reason: enhanced material removal rates caused by generated cavitation bubbles in the liquid.[3] Using liquid processing aids is not common for ultrashort pulse laser machining. The generation of nanoparticles in liquids using such lasers is a very active topic with many publications. There are also publications on ultrashort pulse laser workpiece machining and surface processing of different materials [4], but in total the topic is far from well investigated.

In liquids, ultrashort pulse lasers induce strong non-linear processes leading to bubble formation, instabilities in the intensity distribution, spectral broadening, longer pulse durations and filamentation.[5] The drawbacks resulting from these processes and the complicated handling using a closed process chamber with tubing and circulating pump are the reason for its unattractiveness. The complex interaction processes of laser pulses, liquid and material as well as the limited compatibility of many process observation techniques with in-liquid laser processing is a challenge for process understanding. However, the chaotic laser ablation process in a liquid with highly turbulent flows in the interaction zone is expected to allow for interesting functional surface topographies. This paper shall present our first observations.

2. Experimental setup

Laser processing in liquids is often done in a very simple setup. A droplet of the liquid is placed on the workpiece surface. The laser is focused into this droplet. This quick and dirty method has a few drawbacks. The curved surface of the droplet with, in most cases, unknown and probably changing height leads to a lack of knowledge in focus diameter and height. The laser beam interacts with a rising number of ablated particles and bubbles. Smaller droplets can be ejected and, at worst, deposit on the surfaces of the focusing optics. Such a simple setup is not suitable for longer processing times or investigations with increased requirements on reliability.

To allow for a better process stability and minimized interaction of bubbles and ablated particles with the laser beam, a process chamber has been manufactured. It includes a two inch beam entrance window which is also large enough for on-axis process observation and illumination. Two mutually opposite liquid inlets and outlets with external

tubing and submersible pump in a liquid container allow for operation in circulation mode or single-pass mode with additional collection container. The chamber has been designed for optimized liquid flow without whirls which could otherwise cause backflows of bubbles and particles. The integrated workpiece holder consists of a variable screw clamping which can be adjusted to different distances between workpiece surface and backside of the entrance window which corresponds to the liquid height above the workpiece. The chamber is operated without any air inclusion. Fig. 1 demonstrates how effectively bubbles are removed in the liquid flow. If the pump is switched off, bubbles accumulate below the entrance window already shortly after starting a laser process. If the pump is switched on, long processing times without disturbances are possible.

The liquid used in the experiments presented here was distilled water at room temperature. The water was pumped in circulation mode and changed to fresh water whenever the concentration of ablated particles became visible. The effective flow rate was set to approximately 10l/min at a flow cross-section of 70mm width and 30mm height at the processing area. The liquid content in the whole system was approximately 15l.



Fig. 1. (left) bubble accumulation with pump switched off; (right) no bubbles with pump switched on. The free diameter of the entrance window is 40mm.

For the experiments in water two laser systems have been used. First, a picosecond laser system Hylase-25 from neoLase GmbH (Germany) with a wavelength of 1064nm, <15ps pulse duration, 25W average power and up to 40MHz pulse repetition rate; secondly, a femtosecond laser system Femto Power Compact Pro from Femtolasers Produktions GmbH (Austria) with a central wavelength of 800nm, <30fs pulse duration, 1W average power and 1kHz pulse repetition rate. At the picosecond laser setup a galvo scanner (Scanlabs intellySCAN 14) with 100mm telecentric f-theta lens (Linos) has been used for beam positioning and focusing. At the femtosecond laser setup the process chamber was mounted onto a xyz-positioning system (Pysik Instrumente). Focusing was done with a 140mm achromatic lens (Qioptiq). Both $1/e^2$ focus diameters were measured in air to be 20 μ m using a laser beam profiler (Primes MicroSpotMonitor). The beam quality M^2 was 1.3 for both lasers. Since the estimation of focus diameters in the water filled chamber was found to be not really reliable, we are refraining from calculating laser fluences. Laser pulse energies are given instead.

For setting the laser focus position on the surface of the workpieces an offset to the focus position in air was calculated based on geometric optics and the refractive indices of the entrance window and water. This value was used as a rough start value for an experimental focus search via ablation tests at different focus heights. The repeatability of the sample height when taking the sample out for inspection and placing it back in the chamber again was equal to or better than the uncertainty of the right focus position which was around $\pm 20\mu\text{m}$.

3. Processing of silicon in water

A part of a Si(111) wafer with a thickness of $700\mu\text{m}$ has been cleaned with acetone, clamped onto the workpiece holder and placed inside the processing chamber. The water level between entrance window and workpiece surface was 29.3mm . The laser focus was set on the workpiece surface. A set of ablation experiments was carried out by varying laser pulse energy and pulse numbers. The stage system stopped during exposure. Thus, the pulse overlap was 100%. The experiments described in the following sections have been performed using the femtosecond laser.

3.1. In-water ablation with a single laser pulse

Fig. 2 shows scanning electron microscope (SEM) images with results of single laser pulse exposure with $5\mu\text{J}$ (left) and $50\mu\text{J}$ (right) pulse energy. At low pulse energies a concentric wave-like structure is formed. It consists of a pronounced inner ring and weaker outer rings. Material from the center has been moved outwards. This forms the raised inner ring. The outer rings seem to be formed by compression. Their period is too small for laser-induced ripples caused by plasmons. The plasmon wavelength on silicon in water at a laser wavelength of 800nm is expected to be around 640nm . At higher pulse energies melting is the dominant process. Here, material has been moved outwards in a liquid state. Interestingly, the affected surface area for both results in Fig. 2 is of comparable size.

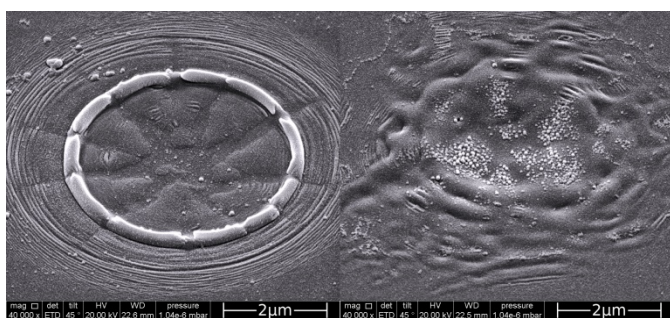


Fig. 2. Single laser pulse ablation on silicon in water; (left) $5\mu\text{J}$ pulse energy; (right) $50\mu\text{J}$ pulse energy. SEM images at 45° tilt angle.

3.2. In-water ablation with a few laser pulses

Fig. 3 shows a typical processing result when applying a few (2..10) laser pulses. Several overlapping concentric wave-like structures appear. It is hard to imagine that this result has

been obtained with a circular laser spot. The overall picture is comparable to interfering waves on the surface of a liquid induced at different points. The point source excitations could be defects in the silicon surface. Every repetition of this experiment resulted in a different pattern of the wave-like structures. From the single pulse results we conclude an actual circular laser spot on the silicon surface.

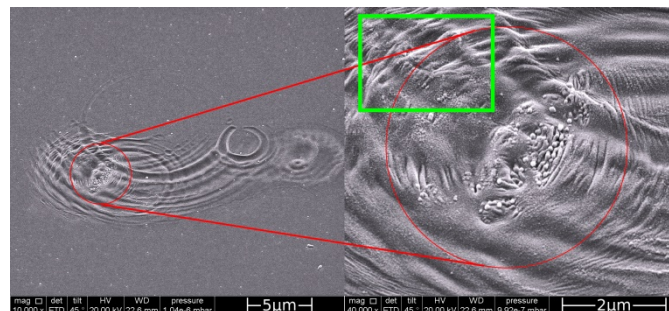


Fig. 3. Silicon ablation in water with five laser pulses at $5\mu\text{J}$ pulse energy; (right) overview; (right) enlarged section. SEM images at 45° tilt angle.

The enlarged section on the right in Fig. 3 shows a second type of wave-like structures with a smaller period. There are curved lines with a period between 300 and 500nm on the right side of the enlarged section. But there are also parallel lines with a period between 500 and 700nm in the green rectangle which corresponds to the plasmon wavelength of 640nm .

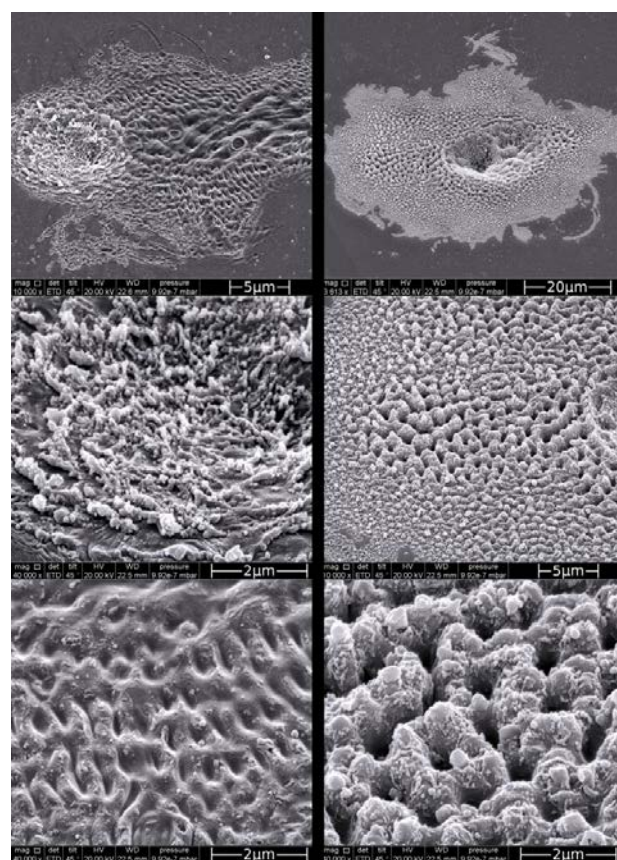


Fig. 4. Silicon ablation in water with (left) 50 laser pulses and (right) 500 laser pulses at $5\mu\text{J}$ pulse energy; enlarged sections in the middle and bottom images. SEM images at 45° tilt angle.

3.3. In-water ablation with many laser pulses

Fig. 4 shows what happens when further increasing the number of laser pulses. With increasing pulse number the overlapping concentric wave-like structures form relatively uniform topographies. Appearance and period are dependent on the local laser fluence. Again, the outline of the whole structure does not reproduce the circular laser spot.

The types of structure which appear are comparable to spike structures which are known from laser processing of silicon and other materials in air. They are also superimposed with nanostructures. The difference when processed in water is the average distance of the spike structures. Sub-micron distances can be seen whereas in air spikes are in a range between 2 and 15 μm . [6]

3.4. Large-area laser patterning in water with femtosecond and picosecond laser pulses

For most applications of surface functionalization larger areas have to be laser patterned. This requires stage movement or laser scanning. For a first test the femtosecond laser has been used. Areas of 2mm \times 1mm have been processed at 6mm/s stage movement and a 6 μm hatch distance. Four sets of parameters have been tested: (R1) one pass in x-direction at 10 μJ pulse energy, (R2) 10 passes alternating in x- and y-direction at 10 μJ , (R3) one pass in x-direction at 20 μJ , and (R4) one pass in x-direction at 200 μJ . Fig. 5 shows an overview of the obtained topographies. Fig. 6 shows enlarged sections. As already seen for the single-spot ablation results, overlapping concentric wave-like structures appear and start forming a topography consisting of sub-micron spikes superimposed with nanostructures. Using higher pulse energy, already single-pass hatching leads to a uniform topography. This allows for short processing times on larger areas.

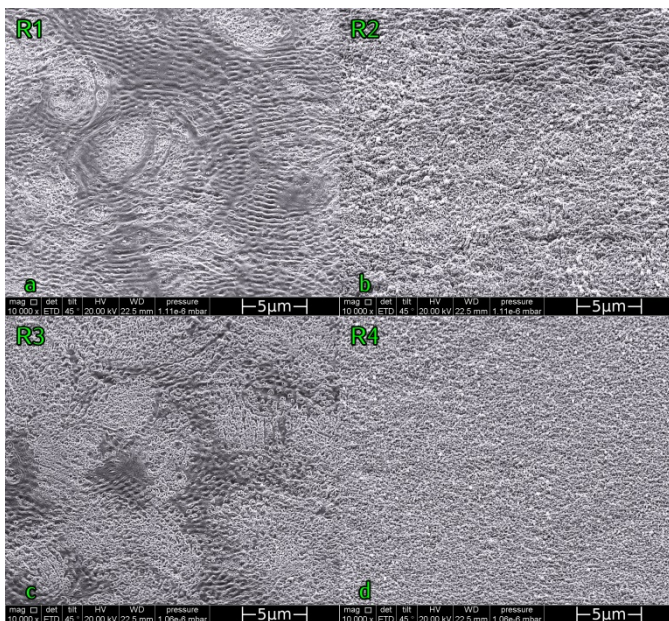


Fig. 5. Processing of larger areas using the femtosecond laser. SEM images at 45° tilt angle.

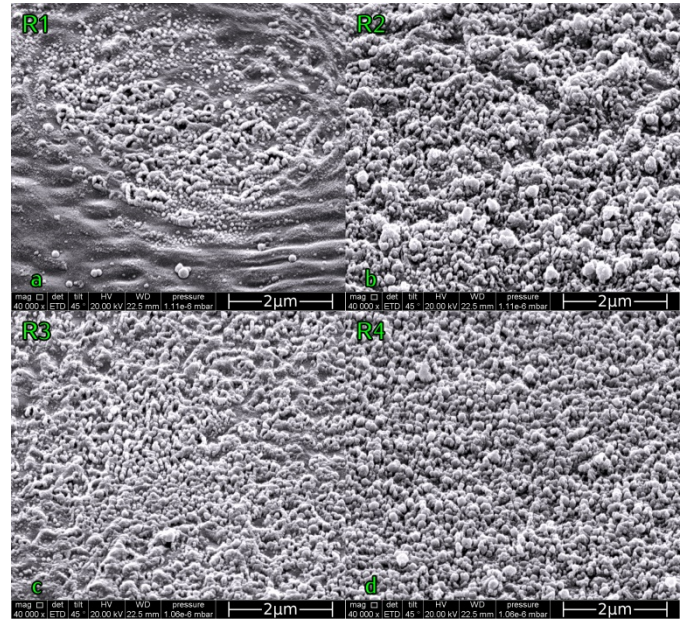


Fig. 6. Enlarged sections of the topographies shown in Fig. 5. SEM images at 45° tilt angle.

For comparison the picosecond laser has been used for the same task. The pulse repetition rate has been set to 50kHz. The scanning velocity has also been increased by a factor of 50. Fig. 7 shows the obtained topography. It totally differs from the topographies which have been obtained using the femtosecond laser. There are no spike structures. Neither there are smoothly solidified liquid flows. The processed surface shows flaking with relatively sharp edges as it can be expected for brittle material.

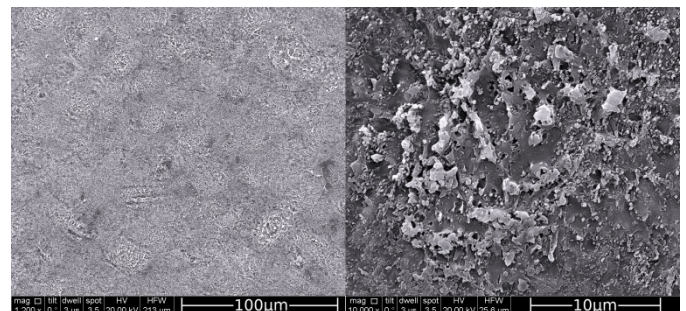


Fig. 7. Silicon surface processing in water using the picosecond laser at 50kHz pulse repetition rate; (left) overview and (right) enlarged section. SEM images at 45° tilt angle.

4. Discussion

The formation of the presented structures on silicon is far from being fully understood. When doing ultrashort pulse laser processing in air, ripple structures are explained by plasmonics. [7, 8] For spike structures there is no generally accepted theory. In water the process is even more complicated. Ultrashort laser pulses induce strong non-linear processes leading to bubble formation, instabilities in the intensity distribution, spectral broadening, longer pulse durations and filamentation. The direct interaction between laser pulse and water as well as the interaction between the rapidly heated material surface and water influences structure

formation. One can distinguish three time scales. The shortest is in the order of the laser pulse duration and affects the laser pulse properties (temporal and spatial intensity distribution as well as spectrum and polarization). The next longer time scale is characterized by property changes of workpiece and liquid materials (temperature, pressure, motion, and composition). These do not influence the laser pulse properties. Many of these changes decay before arrival of the next laser pulse. Ablated particles and bubbles in the liquid can easily interact with the next laser pulse and should therefore be considered on a longer time scale. The water flow in the processing chamber has been found to be fast and laminar enough to minimize the interaction of particles and bubbles with following laser pulses. Laser light diffraction at particles or bubbles as reason for the formation of the concentric wave-like structures is an obvious idea but can be invalidated by the appearance in the single-pulse experiments and by almost unchanged topographies in multi-pulse experiments when longer waiting times between the pulses are introduced.

For plasmonics, the period of the structures is in almost all cases not in a range close to the plasmon wavelength. There were no structures which could clearly be identified as ripple structures.

Shen et al. [9] did ablation experiments of silicon in stagnant water using a femtosecond laser at a wavelength of 400nm. The results are comparable to the results obtained here. In the same paper they report on experiments at 800nm wavelength. These results were not shown in their paper but they describe the structures as totally different from the ones obtained at 400nm and characterized by hole formation. A publication of these results followed in [10]. They obtained two types of ripple structures – micrometer ripples at medium laser fluences and sub-micrometer ripples at low fluences. In both cases the long axis of the ripples was perpendicular to the linear laser polarization. A third class of structures consisting of micrometer structures and sub-micrometer holes was obtained at high laser fluences. No ripples were found on these structures. These three classes of structures were attributed to different types of laser interaction – melting and resolidification without ablation in the low fluence regime, ablation without bubble formation in the medium fluence regime, and ablation with bubble formation in the high fluence regime. Sub-micron ripples were also found in other comparable experiments. [11, 12]

There are a few differences in the experimental conditions of the results presented here. Shen et al. used a sub-surface focus position. The water level above the surface was roughly one third of the water level in our experiments. The pulse duration was 100fs – longer than ours. The pulse energy we used fits to their high fluence regime. In accordance, there are no ripple structures. Shen et al. observe wave-like concentric ring structures in their 400nm experiments but not in their 800nm experiments whereas we see them using a wavelength of 800nm. Our sub-micrometer spike structures are smaller

than the structures obtained by Shen et al. in the high fluence regime. Currently, there is no obvious explanation. Further experiments are necessary. One effect when focusing femtosecond laser pulses in water is depolarization.[13] If this is a possible explanation of ripple suppression at higher laser fluences has to be checked.

5. Conclusion

Laser processing in liquids appears interesting for surface functionalization. For uniform large-area topographies a suitable process chamber with entrance window for the laser beam, filled without air gap, with liquid in- and outlet, and a pump for removing ablated particles and bubbles at constant liquid flow is necessary. Using a femtosecond laser allows for submicron spike structures superimposed with nanostructures. In comparison to ablation in air smaller structures are possible. Ripple structures could not be observed.

References

- [1] Vorobyev AY, Guo C. Direct femtosecond laser surface nano/microstructuring and its applications. *Laser & Photonics Review* 2013; 7:385-407.
- [2] Koch J, Korte F, Fallnich C, Ostendorf A, Chichkov BN. *Opt Eng* 2005; 44(5):051103.
- [3] Sajti CL, Sattari R, Chichkov B, Barcikowski S. Ablation efficiency of α -Al₂O₃ in liquid phase and ambient air by nanosecond laser irradiation. *Appl Phys A* 2010; 100(1):203-206.
- [4] Bärsch N, Werelius K, Barcikowski S, Liebana F, Stute U, Ostendorf A. Femtosecond laser microstructuring of hot-isostatically pressed zirconia ceramic. *Journal of Laser Appl* 2007; 19(2):107.
- [5] Schaffer CB, Nishimura N, Glezer EN, Kim AM-T, Mazur E. Dynamics of femtosecond laser-induced breakdown in water from femtoseconds to microseconds. *Opt Exp* 2002; 10(3):196-203.
- [6] Fadeeva E, Schlie S, Koch J, Ngezhahayo A, Chichkov BN. The hydrophobic properties of femtosecond laser fabricated spike structures and their effects on cell proliferation. *Pys Status Solidi A* 2009; 206(6):1348-1351.
- [7] Sipe JE, Young JF, Preston JS, Vandriel HM. Laser-induced periodic surface structure. 1. Theory. *Phys Rev B* 1983; 27:1141-1154.
- [8] Bonse J, Höhm S, Kirner SV, Rosenfeld A, Krüger J. Laser-induced periodic surface structures – a scientific evergreen. *IEEE Journal of Selected Topics in Quantum Electronics* 2017; 23(3)
- [9] Shen MY, Crouch CH, Carey JE, Mazur E. Femtosecond laser-induced formation of submicrometer spikes on silicon in water. *Appl Phys Lett* 2004; 85:5694.
- [10] Shen M, Carey JE, Crouch CH, Kandyla M, Stone HA, Mazur E. High-density regular arrays of nanometer-scale rods formed on silicon surfaces via femtosecond laser irradiation in water. *Nano Lett* 2008; 8(7):2087-2091.
- [11] Wang C, Huo H, Johnson M, Shen M, Mazur E. The thresholds of surface nano-/micro-morphology modifications with femtosecond laser pulse irradiations. *Nanotechnology* 2010; 21:075304.
- [12] Straub M, Afshar M, Feili D, Seidel H, König K. Periodic nanostructures on Si(100) surfaces generated by high-repetition rate sub-15 fs pulsed near-infrared laser light. *Opt Lett* 2012; 37(2):190-192.
- [13] Yu J, Jiang H, Wen J, Yang H, Gong Q. Mechanism of depolarization of white light generated by femtosecond laser pulse in water. *Opt Exp* 2010; 18(12):12581-6.